Acta Biomaterialia 80 (2018) 58–65

Contents lists available at ScienceDirect

Acta Biomaterialia

journal homepage: www.elsevier.com/locate/actabiomat

Full length article

Design of DNA-based innovative computing system of digital comparison

Chunyang Zhou [a], Hongmei Geng [a], Chunlei Guo [a,b,*]

[a] The Guo China-US Photonics Laboratory, Changchun Institute of Optics, Fine Mechanics and Physics, Chinese Academy of Sciences, Changchun, Jilin 130033, PR China
[b] The Institute of Optics, University of Rochester, Rochester, NY 14627, USA

ARTICLE INFO

Article history:
Received 18 April 2018
Received in revised form 20 August 2018
Accepted 12 September 2018
Available online 15 September 2018

Keywords:
Digital comparator system
Graphene oxide
DNA
Logic gate
Computing

ABSTRACT

Despite great potential and extensive interest in developing biomolecule-based computing, the development of even basic molecular logic gates is still in its infancy. Digital comparator (DC) is the basic unit in traditional electronic computers, but it is difficult to construct a system for achieving large-scale integration. Here, we construct, for the first time, a novel logic computing system of DCs that can compare whether two or more numbers are equal. Our approach is by taking advantage of facile preparation and unique properties of graphene oxide and DNA. The DC system reported in this work is developed by the DNA hybridization and effective combination of GO and single-stranded DNA, which is regarded as the reacting platform. On the basis of this platform and reaction principle, we have developed 2-inputs, 3-inputs, and 4-inputs DCs to realize the comparison of two or more binary numbers. We predict that such a state-of-the-art logic system enables its functionality with large-scale input signals, providing a new direction toward prototypical DNA-based logic operations and promoting the development of advanced logic computing.

Statement of Significance

The overarching objective of this paper is to explore the construction of a novel DNA computing system of digital comparator driven by the interaction of DNA and graphene oxide (GO). GO can efficient bind the dye-labeled, single-stranded DNA probe and then quench its fluorescence. In the case of the target appearing, specific binding between the single-stranded probe and its target occurs, changing the conformation and relationship with GO, then restoring the fluorescence of the dye. We have developed the 2-inputs, 3-inputs, and 4-inputs digital comparator circuits, which are expected to realize the comparison of large-scale input signals and can avoid the problems of design complexity and manufacturing cost of integrated circuits in traditional computing.

1. Introduction

As one of the basic unit of a digital system, digital comparator (DC) is used to compare the two or more binary numbers or determine whether they are equal. In traditional electronic computers, the DC circuits that compare inputs and determine if they are equal or not could be realized by an XNOR gate or an XOR gate. However, for digital comparators with large input signals, a greater number of transistors and more complicated logic circuit connections should be needed, which greatly increases the design complexity and manufacturing cost of the integrated circuit [1]. Not only that, with the increasing number of input signals to a certain value, the speed and quality of the circuit will be affected since such big data that processed by the electronic computer is limited. To solve these problems, the biomolecule-based logic circuits came into being [2]. The fascinating discovery that biomolecules and their inherent conversions could use logic operations for information transmission and processing [2], just like the human brain or electronic computer, has spawned considerable research into intelligent decision-making, molecular-level logic devices [3–5]. Such revelations have shown great applications potentially, especially in the field of life science, medical diagnostics [6], biosensing [7,8] and data storage [9,10], improving the understanding of complex biological phenomena in humans [11]. With the reliable prediction

* Corresponding author at: The Guo China-US Photonics Laboratory, Changchun Institute of Optics, Fine Mechanics and Physics, Chinese Academy of Sciences, Changchun, Jilin 130033, PR China.
E-mail address: cyzhou@ciomp.ac.cn (C. Guo).

https://doi.org/10.1016/j.actbio.2018.09.018
1742-7061/

of hybridization behavior based on the Watson-Crick base-pairing principle, DNA is endowed with excellent advantages for the construction of biomolecular computing systems [12–14]. Its simple synthesis method, predictable molecular behavior, and good biological compatibility can largely reduce operating costs, facilitate practical operations *in vivo* and *in vitro*, and also provide the potential for the construction of information processing systems [15].

Graphene is a one-atom thick 2D nanomaterial with distinguished electronic, thermal and optical properties [16–20]. Its derivative, graphene oxide (GO), could serve as great support for biomolecules due to its flake structure, large surface area, and rich π-π conjugation property [21]. GO can efficient bind the dye-labeled, single-stranded DNA probe and then quench its fluorescence [22–24]. In the case of the target appearing, specific binding between the single-stranded probe and its target occurs, changing the conformation and relationship with GO, then restoring the fluorescence of the dye [25,26]. Such designated GO/DNA interaction could fulfill significant applications in the development of biosensing [27]. In addition, the multifunctional GO/DNA interaction has been widely used to realize various basic logic gates, such as OR, AND, XOR, NOR, INHIBIT, and advanced logic gates, such as full adder, full subtractor, half adder, half subtractor, reversible logic gate, and ternary logic circuits, etc [28–34]. However, to fulfill the requirements for the rapid development of biomolecular computation, there is high demand to design and construct versatile logic devices with the ability to perform multiple operations. Previous works in digital comparators have only realized the most basic one-bit binary number comparison, due to the limitation of the reaction substrate and input signals [35,36]. Similar to traditional computers, the previously demonstrated comparators cannot realize digital comparison of large-scale binary numbers. In this work, by taking advantage of the unique GO/DNA platform, for the first time, we explored new utilization of DNA candidates from the consideration of digital comparator logic system construction. The 2-1, 3-1, and 4-1 DC has been successfully realized based on the same platform of GO/DNA. Therefore, such prepared computing systems of DC is predicted to solve the big data issues according to the hybridization behavior based on the Watson-Crick base-pairing principle, and then avoid the problems of design complexity and manufacturing cost of integrated circuits in traditional computing.

2. Experimental

2.1. Materials and instruments

All the DNA sequences used in this work were purchased from Sangon Biotechnology Company (Shanghai, China) and were listed in Table S1. Other chemicals were of reagent grade and used without further purification. The DNAs were quantified by UV–Vis absorption spectroscopy (Cary Series Scan UV/Vis/NIR Spectrophotometer from Agilent Technologies) with the following extinction coefficients (ε260 nm, M^{-1} cm^{-1}): A = 15400, G = 11500, C = 7400, T = 8700. A Cary Eclipse Fluorescence Spectrophotometer from Agilent Technologies was used to collect the fluorescence emission spectra of GO/P complexes in Tris-HCl buffer (20 mM Tris-HCl, 200 mM KCl, 10 mM $MgCl_2$, pH 8.0) under room temperature by irradiating FAM at 494 nm.

2.2. Preparation of GO

Graphene oxide was synthesized by a modified Hummers method [37]. Briefly, the mixture of graphite powder (5 g), P_2O_5 (5 g), $K_2S_2O_8$ (5 g) was first added to H_2SO_4 (98%, 35 mL). Then,

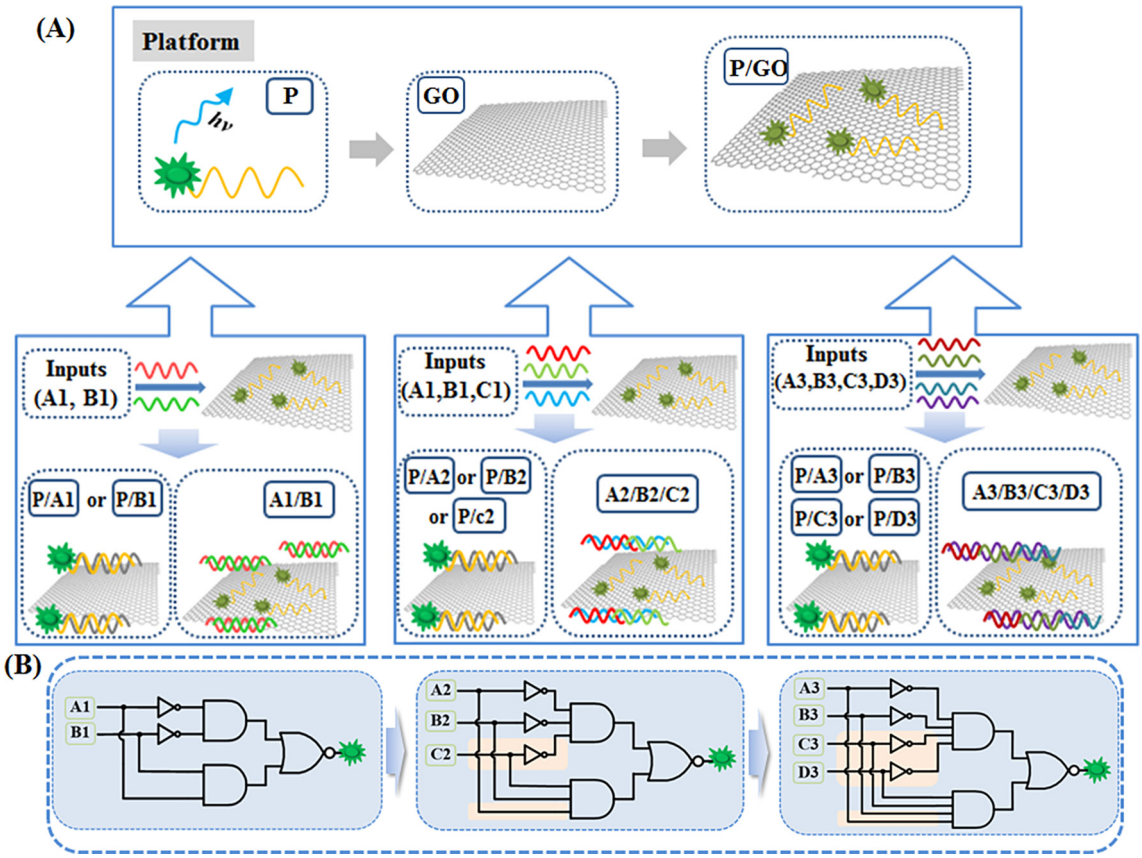

Scheme 1. The operation principle and equivalent circuits of the designed DC system based on DNA hybridization.

the mixture was heated to 80 °C for 4 h under constant stirring and cooled down. After the addition of water, the product was collected and centrifuging and then filtered to remove the acid. Next, The precipitate was redissolved in H_2SO_4 and the $KMnO_4$ (30 g) was added under constant stiring. After 24 h, the 1200 mL of H_2O was added and stirred for 3 h. Finally, after the addition of H_2O_2 (35%, 40 mL), the color of the mixture changed to yellow. The product was filtered and washed with HCl and H_2O, and then loaded in dialysis tubes and purified for 2 weeks to remove any remaining metal.

2.3. Statistical analysis

Before the operation of all the logic gates, the optimized condition should be confirmed during the hybridization of DNAs. First of all, the optimized concentration of GO that can absorb P (100 nM) on its surface was demonstrate to be 7 μg/mL. The fluorescence of FAM modified P could be decreased when absorb on the surface of GO for FRET as shown in Fig. S1. Next, the optimized concentration of hybridizations between the input (A1 and B1) and P for the operation of 2-1 DC were confirmed as shown in Fig. S2. Based on the fluorescence intensity of P, the optimized concentration of A1, B1 and A1:B1 were 350 nM, 300 nM and 1:1. Then, the optimized hybridizations for the operations of 3-1 and 4-1 DC were also confirmed as show in Figs. S3 and S4.

2.4. Logic gates operation

The DNA sequences were dissolved in water as stock solution and diluted with Tris-HCl buffer for hybridization in the logic circuits. After the optimization of inputs and GO/P platforms, the optimized concentration of inputs were added to the platform and incubated under room temperature for 30 min. The fluorescence output signals were then recorded and the corresponding thresholds were defined to implement the function of the digital 2-1, 3-1 and 4-1 comparator system.

2.5. Native polyacrylamide gel electrophoresis (PAGE)

Before use, the DNA stock solutions were diluted to 2 μM with Tris-HCl buffer and heated at 90 °C for 10 min. After cooled down to room temperature slowly, the desired volume of the platforms and their respective inputs were mixed and incubated for 30 min. After the preparation of 30% native polyacrylamide gel, the electrophoresis was conducted in 1× TBE (17.8 mM Tris, 17.8 mM boric acid, 2 mM EDTA, pH 8.0) at a constant voltage of 120 V for about 1 h. Finally, the finished gels were scanned by a UV transilluminator after staining with Gel-dye.

3. Results and discussion

The operation mechanism of the DC system is illustrated in Scheme 1. The DC logic system requires different inputs (two inputs of A1 and B1 for 2-1 DC, three inputs of A2, B2, and C2 for 3-1 DC and four inputs of A3, B3, C3, and D3 for 4-1 DC) and a 6-carboxyfluorescein (FAM, emission max at 520 nm) fluorescent signal as output. As shown in Scheme 1a, the FAM modified single-stranded P can be adsorbed on the surface of GO (GO/P) since GO contains the unique property of performing high affinity with single-stranded DNA through π-π stacking interactions, and quench the FAM fluorescence by fluorescent resonance energy transfer (FRET). Such GO/P platform was regarded as the reacting platform to realize the DC logic system. In order to demonstrate the application prospects of the GO/P platform and finally achieve the system of DC, we need to proceed from the most basic, which should be first realized for the comparison of two binary input sig-

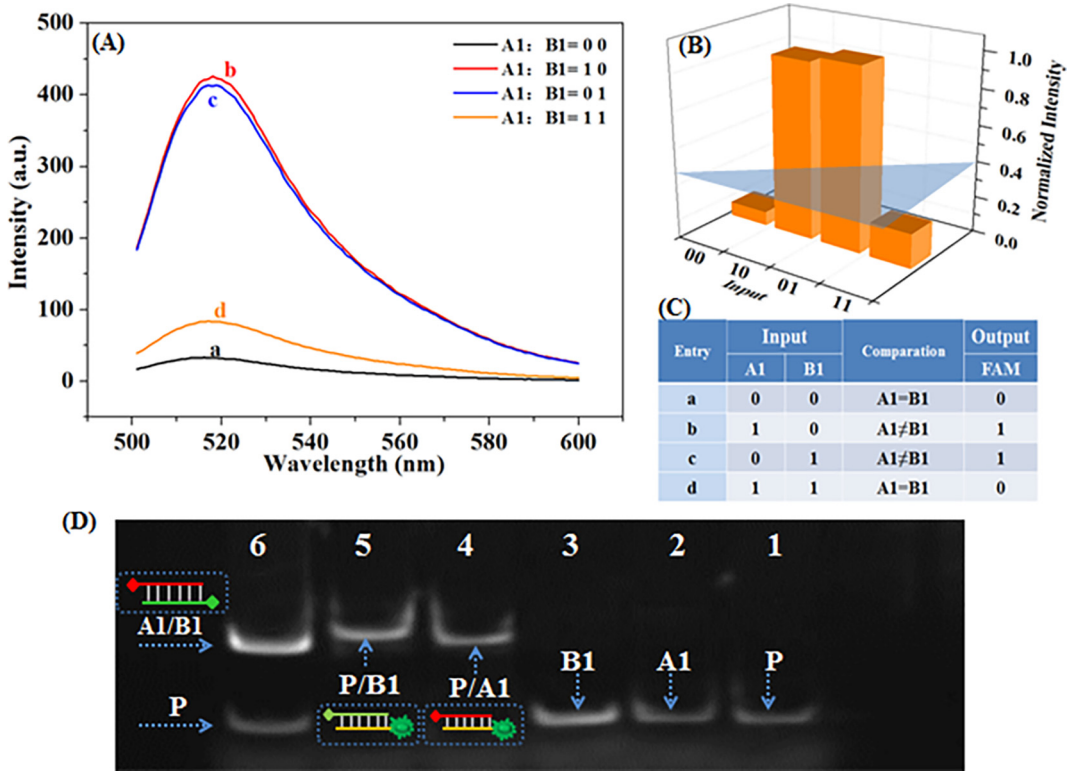

Entry	Input		Comparation	Output
	A1	B1		FAM
a	0	0	A1=B1	0
b	1	0	A1≠B1	1
c	0	1	A1≠B1	1
d	1	1	A1=B1	0

Fig. 1. (a) The intensity of output fluorescence signals of FAM and (b) its corresponding histogram of the normalized fluorescence responses for the 2-1 digital comparator operation triggered by different input combinations. (c) The truth table for the 2-1 digital comparator. (d) PAGE analysis of the 2-1 digital comparator. Different DNA samples were added into lanes 1–6. Lane 1: P, Lane 2: A1, Lane 3: B1, Lane 4: P + A1, Lane 5: P + B1, Lane 6: P + A1 + B1.

nals shown in Scheme 1A. As shown in Scheme 1B, the equivalent circuits of 2-1, 3-1 and 4-1 DC had been realized by logic gates in electronic circuits. During these circuits, with the increasing number of input signals, logic devices need to be added continuously. When the logic devices are increased to a certain value, the speed and quality of the circuit will be affected since such large data that can be processed by the electronic computer is limited. However, in DNA-based biocomputing system, by designing DNA sequences and platform, it is possible to achieve its function in a relatively short time simply by adding DNA inputs, which greatly overcomes the problem of large data encountered in electronic circuits and increase the progress efficiency. When the system increased to a n-put comparator, the n DNA sequences could be added to the solution, replacing the work of electronic devices by high-efficient hybridization between DNA, providing a promising future for the development of biocomputing.

3.1. Operation of 2-1 digital comparator

The principle of the GO/P platform-based system to perform the 2-1 DC was shown in Scheme 1A. The TEM and absorbance spectrum of GO were shown in Fig. S1. Furthermore, the pH value and buffer concentration were optimized for the operation of DC system as shown in Fig. S2. To establish optimal conditions for the DC, different concentrations of inputs were discussed with GO/P platform as shown in Figs. S3–S5. The FAM-labeled P that absorbed on the surface of GO was utilized as the reaction platform. From the truth table shown in Fig. 1C we can get that, for input signals, the absence of input DNA strands were set as "0", otherwise, they were set as "1" for their presence. Only when two input signals exist or not at the same time, can the two binary digits be equal, otherwise they are not equal. Thus in the absence of inputs, the P anchored on the surface of GO with low fluorescent signal quenched by GO via FRET as shown in Fig. 1A, curve a. Such low fluorescence was defined as "0", with the mean of A1 equal to B1. However, the single-stranded DNA adsorption on GO is reversible, and also, the adsorbed single-stranded DNA can be desorbed from GO by adding the corresponding complementary DNA to form the duplex as the affinity of duplex on GO is much weaker than that of single-stranded DNA. So when A1 is added to the platform, it can hybridize with P and form the duplex of P/A1 and then desorb from the surface of GO, recovering a strong fluorescence emission at 520 nm (Fig. 1A, curve b) defined as "1" for indicating that the two binary codes were not equal. Same as above, when B1 was added to the platform, it can also hybridize with P and form the duplex of P/B1, performing a strong fluorescence as shown in Fig. 1A, curve c. However, when A1 and B1 were all present, they have the priority to hybridize with each other and form the duplex of A1/B1, leaving P alone on the surface of GO and performing a low fluorescence (Fig. 1A, curve d). Similar to the approach applied in electronic circuits, the output threshold values were defined in this work. First of all, the fluorescent responses of FAM at 520 nm were normalized and plotted as column bar shown in Fig. 1B, producing the corresponding truth table shown in Fig. 1C. The output threshold value was defined as "1" when the normalized fluorescence intensity was higher than 0.4. On the contrary, the output thresh-

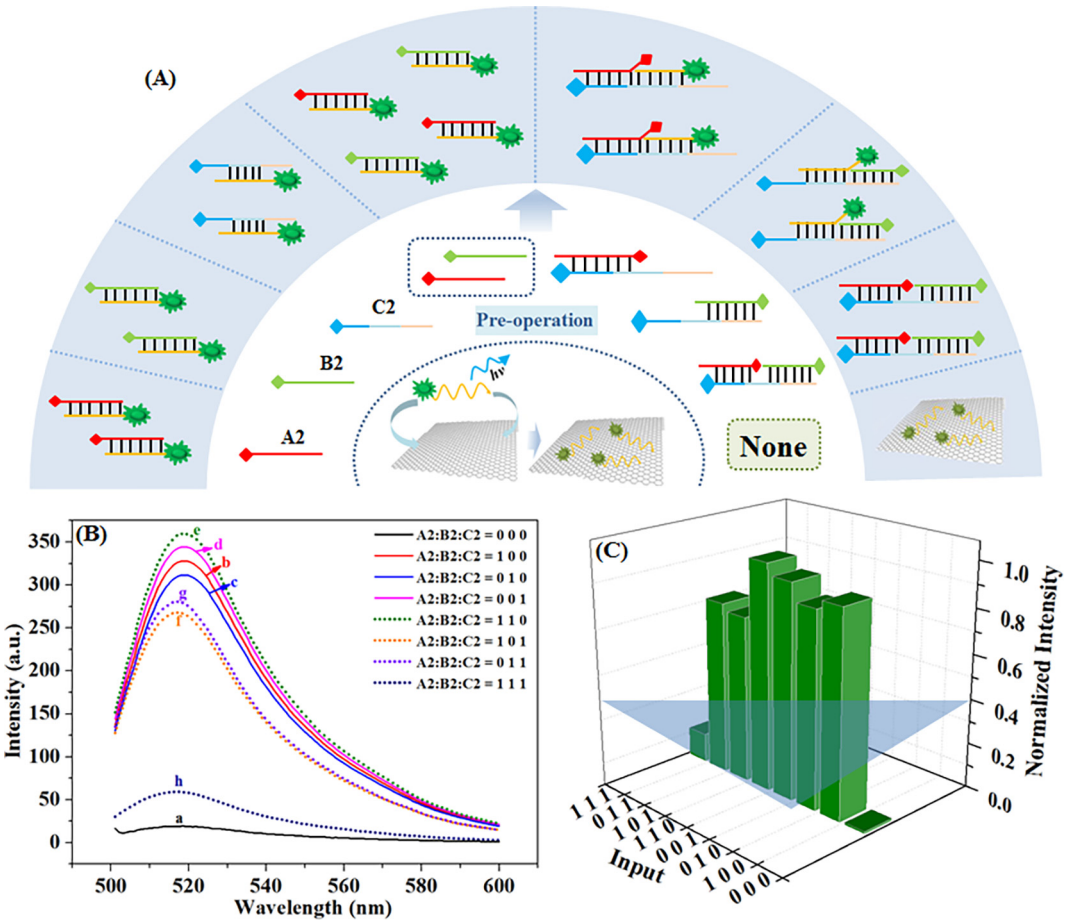

Fig. 2. (A) The pre-operation and operation of different inputs with the platform of GO/P for the operation of 3-1 DC, which corresponds to the truth table shown in Fig. S5. (B) The intensity of output fluorescence signals of FAM and (C) its corresponding histogram of the normalized fluorescence responses for the 3-1 digital comparator operation triggered by different input combinations.

old value can be defined as "0" when the normalized fluorescence intensity was lower than 0.4.

As shown in Fig. 1D, the native polyacrylamide gel electrophoresis (PAGE) experiments were performed to identify the DNA hybridizations during the 2-1 DC operations. The DNAs contained in different belts have been determined. From Lane 1 to Lane 3, the bands showed the individual single-stranded DNA strands of P, A1 and B1, which appeared at a similar positions. Upon the addition of A1 to P, a new belt appeared in Lane 4, indicating the formation of duplex P/A1. For the same reason, when the addition of B1 to P, a new band that represented the hybridization of P and B1 was appeared. However, in the presence of A1 and B1, a new band appeared at a new position, which means the prior hybridization of A1 and B1, forming the duplex of A1/B1 and leaving the singe-stranded P alone at the lower position of Lane 6. All the above proved the interactions between different strands were in accord with the reasonable design of 2-1 DC.

3.2. Operation of 3-1 digital comparator

After the operation of 2-1 DC, the 3-1 DC logic circuit was conceptually performed, into which the third input of C2 was introduced to properly mimic its function of comparing the equality of the three inputs as shown in Fig. 2A. Its corresponding truth table was presented in Fig. S5. To testify the feasibility of our strategy, verification experiments were explored as shown in Fig. 2B. First of all, the realization of the 3-1 DC was still based on the platform of GO/P. As shown in Fig. 2A, in the presence of A2, B2, or C2, they all can hybridize with P and release the FAM fluorescence from the surface of GO, obtaining a high fluorescence signal shown in Fig. 2B, curve b, c and d. In addition, when A2 and B2 were added to the platform, they all can hybridize with P and also perform a high fluorescence signal as shown in Fig. 2B, curve e. The designed single-stranded C2 can not only hybridize with P, but also with A2 and B2. Thus, the duplex of C2/A2 was formed before the addition

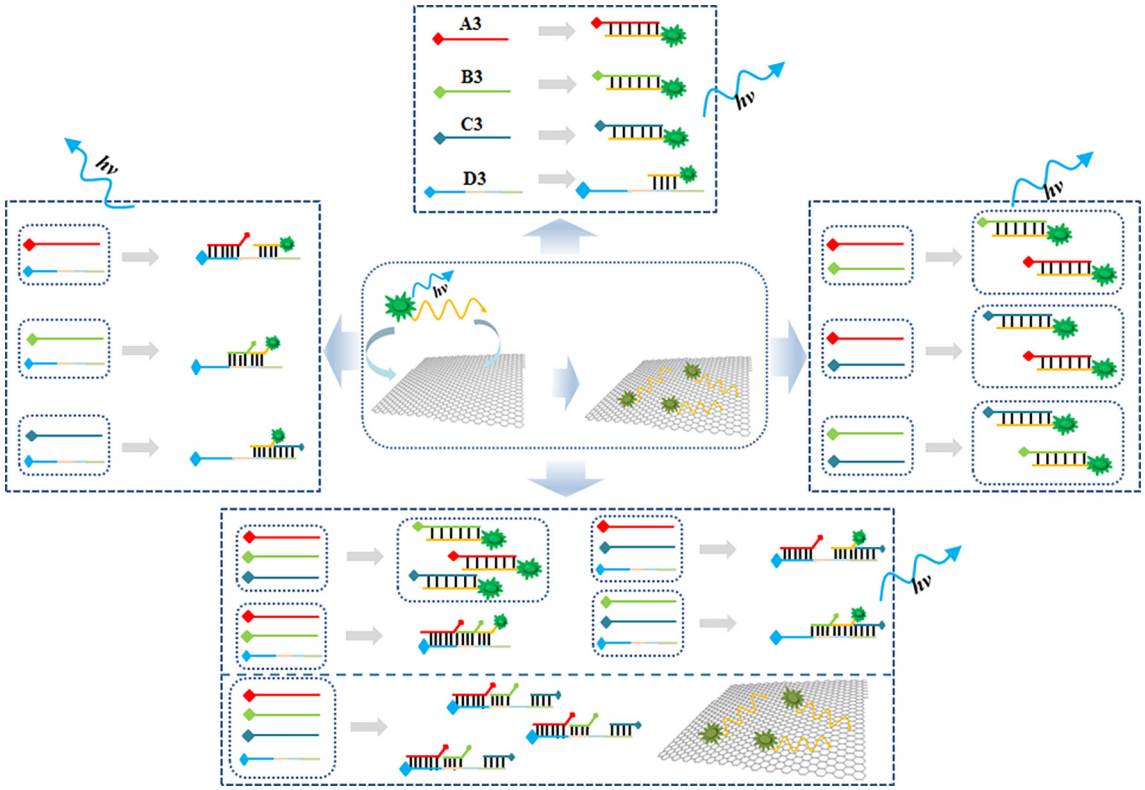

Fig. 3. The reaction mechanism of different input DNAs with GO/P platform for 4-1 DC.

Inputs				Comparation	Output	Platform	Inputs				Comparation	Output
A3	B3	C3	D3				A3	B3	C3	D3		
0	0	0	0	A3=B3=C3=D3	0	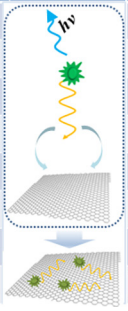	0	1	1	0	A3≠B3=C3≠D3	1
1	0	0	0	A3≠B3=C3=D3	1		0	1	0	1	A3≠B3≠C3≠D3	1
0	1	0	0	A3≠B3=C3=D3	1		0	0	1	1	A3=B3≠C3=D3	1
0	0	1	0	A3=B3≠C3=D3	1		1	1	1	0	A3=B3=C3≠D3	1
0	0	0	1	A3=B3=C3≠D3	1		1	1	0	1	A3=B3≠C3≠D3	1
1	1	0	0	A3=B3≠C3=D3	1		1	0	1	1	A3≠B3=C3=D3	1
1	0	1	0	A3≠B3≠C3≠D3	1		0	1	1	1	A3≠B3=C3=D3	1
1	0	0	1	A3≠B3=C3≠D3	1		1	1	1	1	A3=B3=C3=D3	0

Fig. 4. Truth table of the 4-1 digital comparator logic operation.

of A2 and C2 to the platform, and then the duplex of C2/(P + A2) could be formed with a high fluorescence signal after the addition of the duplex of C2/A2 to the platform, Fig. 2B, curve f. With the same reason, as shown in Fig. 2B, curve g, when the addition of the duplex of C2/B2 to the platform, the duplex of C2/(P + B2) with a high fluorescence signal also formed. These high fluorescence signals indicated that the three binary codes were not equal. When all three inputs of A2, B2, and C2 are added to the platform, C2 has the priority to hybridize with both A2 and B2 and then form the duplex of C2/(A2 + B2), leaving P alone on the surface of GO and performing a low fluorescence as shown in Fig. 2B, curve h, indicating that the three binary codes were equal. Therefore, the experiment results have proven the feasibility of our strategy for the operation of a 3-1 DC logic circuit. The fluorescent responses of FAM at 520 nm were thus normalized and plotted as a column bar shown in Fig. 2C. The output threshold value is defined as "1" when the normalized fluorescence intensity is higher than 0.4. On the contrary, the output threshold value can be defined as "0" when the normalized fluorescence intensity is lower than 0.4. To further demonstrate the successful realization of 3-1 DC circuit, the PAGE experiment was also verified as shown in Fig. S6.

3.3. Operation of 4-1 digital comparator

Based on the above mechanism, to show the promising realization of the DC system with large-scale inputs in the future, a 4-1 DC was conceptually operated, into which the fourth input of D3 was introduced as shown in Fig. 3. The corresponding truth table was presented in Fig. 4. The realization of 4-1 DC was also based on the platform of GO/P, which maintained a low fluorescence as shown in Fig. 5A, curve a, indicating the four binary codes were equal. As shown in Fig. 3, when each of the input DNA sequences were added to the platform, hybridizations happened and took P away from the surface of GO, forming the duplex of P/A3, P/B3, P/C3, and P/D3, and exhibiting high fluorescence signals shown in Fig. 5A, curve b, c, d, and e, indicating the four binary codes were not equal. The designed single-stranded D3 can not only hybridize with P, but also with A3, B3, and C3. Thus, when the inputs contained D3 (A3 and D3, B3 and D3, C3 and D3, A3, B3 and D3, A3, C3 and D3, B3, C3, and D3) and were added to the platform, the duplex DNA (D3/(A3 + P), D3/(B3 + P), D3/(C3 + P), D3/(A3 + P + B3), D3/(A3 + P + C3), D3/(B3 + P + C3)) formed and showed high fluorescence signals as shown in Fig. 5A, curve h, j, k, m, n, and o. When A3 and B3 were added to the P/GO, P could hybridize with both of them and demonstrated a high fluorescence as shown in Fig. 5, curve f. When A3 and C3 were added, the duplexes of P/A3 and P/C3 were formed and showed a high fluorescence signal, for the same reason (Fig. 5, curve g). When the B3 and C3 were added to the platform, the duplexes of P/B3 and P/C3 were formed and also showed a high fluorescence signal (Fig. 5, curve i). When A3, B3, and C3 coexist, a high fluorescence signal can also exist as shown in Fig. 5A, curve l. However, when all the four inputs were added to the platform, the D3 have the priority to hybridize with A3, B3, and C3 at the same time, thus leaving P alone on the surface of GO and performing a relative low fluorescence signal as shown in Fig. 5, curve p, which indicates that the four binary codes were equal. Therefore, the experiment results have proven the feasibility of our strategy for the operation of a 4-1 DC logic circuit. The fluorescent responses of FAM at 520 nm were thus normalized and plotted as a column bar shown in Fig. 5B. The output threshold

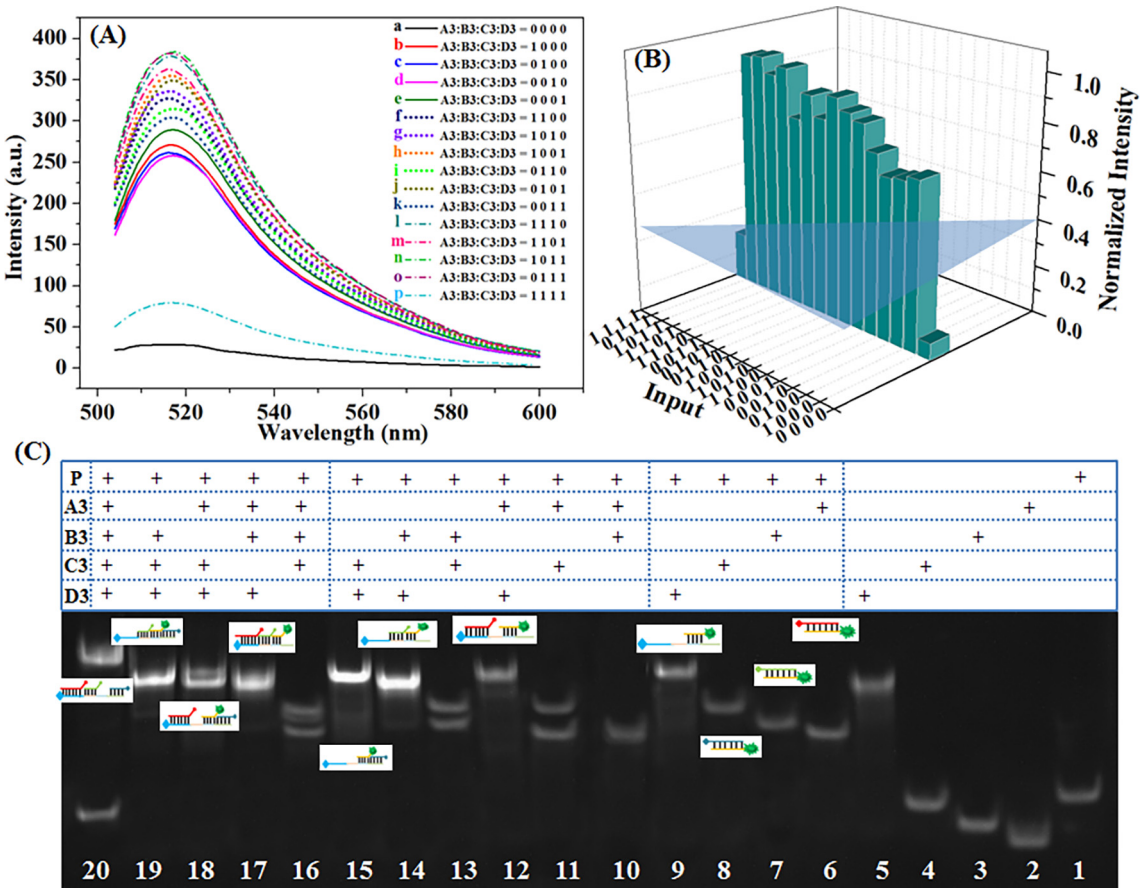

Fig. 5. (a) The intensity of output fluorescence signals of FAM and (b) its corresponding histogram of the normalized fluorescence responses for the 4-1 digital comparator operation triggered by different input combinations. (c) PAGE analysis of the 4-1 digital comparator. Different DNA samples were added into lanes 1–20.

value is defined as "1" when the normalized fluorescence intensity is higher than 0.4. On the contrary, the output threshold value can be defined as "0" when the normalized fluorescence intensity is lower than 0.4.

The hybridizations between different inputs and P strand were also verified for the operation of 4-1 DC by PAGE experiment. As shown in Fig. 5C, the DNA bands of P, A3, B3, C3, and D3 appeared at different positions from Lane 1 to Lane 5. After adding A3, B3, C3, or D3 to P, new bands appeared in Lane 6, Lane 7, Lane 8, and Lane 9, respectively, indicating the duplex formation of P/A3, P/B3, P/C3, and P/D3. In the presence of P, A3, and B3, two new, overlapping bands appeared at the higher positions in Lane 10, indicating the formation of duplexes P/A3 and P/B3. The same phenomenon occurred with the co-existence of A3 and C3, or B3 and C3, producing two new bands as shown in Lane 11 and Lane 13. When A3 and D3 is added to P, D3 can hybridize with both A3 and P, forming a new band in Lane 12 that is the duplex of D3/(P + A3). The situations were the same when B3 and D3, or C3 and D3 were added to P as shown in Lane 14 and Lane 15. In the presence of P, A3, B3, and C3, the formation of new bands showed the duplex of P/A3, P/B3 or P/C3 in Lane 16. In the presence of P, A3, B3, and D3, a new band appeared at a higher position in Lane 17, which was the duplex of D3/(P + A3 + B3). Similarly, the new bands that appeared in Lane 18 and Lane 19 were the duplex of D3/(P + A3 + C3) and D3/(P + B3 + C3). However, with the co-existence of A3, B3, C3, and D3 in P, two bands appeared: the first, higher one was the duplex of D3/(A3 + B3 + C3) and the other was the position of P. Thus, the PAGE results of 4-1 DC were consistent with theoretical design, which fully demonstrated a reliable biomolecular device.

4. Conclusion

In conclusion, for the first time, a logic computing system of digital comparator for comparing whether two or more numbers are equal was successfully fabricated in an enzyme-free condition by integration of GO and DNA as a universal platform. The logic operations were simply based on the DNA hybridization, which offered a cost-effective, operation-simple, and highly repeatable method for the construction of an advanced logic system. Based on such universal platform of GO/P, the 2-1, 3-1, and 4-1 DC were realized the function of comparing whether two or more binary codes are equal. The three realized kinds of digital comparator logic circuits laid the foundation for the development of a DC system, which enables its functionality with large-scale input signals, providing a new field of vision toward prototypical DNA-based logic operations and promoting the development of advanced logic circuits.

Acknowledgements

This work was supported by the National Key Research and Development Program of China (2017YFB1104700), The Natural Science Foundation of China (NSFC, 21404015, 61774155, 61705227) and Jilin Science and Technology Department Project (20150204019GX).

Conflicts of interest

The authors declare that they have no competing interests.

Appendix A. Supplementary data

Supplementary data to this article can be found online at https://doi.org/10.1016/j.actbio.2018.09.018.

References

[1] J.R. Rubens, G. Selvaggio, T.K. Lu, Synthetic mixed-signal computation in living cells, Nat. Commun. 7 (2016) 11685.
[2] P.A. de Silva, N.H.Q. Gunaratne, C.P. McCoy, A molecular photoionic AND gate based on fluorescent signaling, Nature 364 (6432) (1993) 42–44.
[3] Y. Benenson, Biomolecular computing systems: principles, progress and potential, Nat. Rev. 13 (7) (2012) 455–468.
[4] L.M. Adleman, Molecular computation of solutions to combinatorial problems, Science 266 (5187) (1994) 1021–1024.
[5] Y. Benenson, B. Gil, U. Ben-Dor, R. Adar, E. Shapiro, An autonomous molecular computer for logical control of gene expression, Nature 429 (6990) (2004) 423–429.
[6] B. Gil, M. Kahan-Hanum, N. Skirtenko, R. Adar, E. Shapiro, Detection of multiple disease indicators by an autonomous biomolecular computer, Nano Lett. 11 (7) (2011) 2989–2996.
[7] K. Rinaudo, L. Bleris, R. Maddamsetti, S. Subramanian, R. Weiss, Y. Benenson, A universal RNAi-based logic evaluator that operates in mammalian cells, Nat. Biotechnol. 25 (7) (2007) 795–801.
[8] J.K. Arnbratt, M. Hammarson, S. Li, H.L. Anderson, B. Albinsson, J. Andreasson, Photochromic supramolecular memory with nondestructive readout, Angew. Chem. 49 (10) (2010) 1898–1901.
[9] R. Gaber, T. Lebar, A. Majerle, B. Ster, A. Dobnikar, M. Bencina, R. Jerala, Designable DNA-binding domains enable construction of logic circuits in mammalian cells, Nat. Chem. Biol. 10 (3) (2014) 203–208.
[10] K. He, Y. Li, B. Xiang, P. Zhao, Y. Hu, Y. Huang, W. Li, Z. Nie, S.Z. Yao, A Universal platform for building molecular logic circuit based on a reconfigurable three-dimensional DNA nanostructure, Chem. Sci. 6 (6) (2015) 3556–3564.
[11] J. Elbaz, O. Lioubashevski, F. Wang, F. Remacle, R.D. Levine, I. Willner, DNA computing circuits using libraries of DNAzyme subunits, Nat. Nanotechnol. 5 (6) (2010) 417–422.
[12] M. Lin, J. Xu, D. Zhang, Z. Chen, X. Zhang, Z. Cheng, Y. Huang, Y. Li, Scaling up digital circuit computation with DNA strand displacement cascades, J. Theor. Comput. Chem. 332 (6034) (2010) 246–253.
[13] R.J. Lipton, DNA solution of hard computational problems, Science 268 (52) (1995) 542–545.
[14] M. Rana, E.E. Augspurger, M.S. Hizir, E. Alpa, M.V. Yigit, Molecular logic gate operations using one-dimensional DNA nanotechnology, J. Mater. Chem. C 6 (2018) 452–455.
[15] A.K. Geim, K.S. Novoselov, The rise of graphene, Nat. Mater. 6 (3) (2007) 183–191.
[16] N.A. Kotov, Materials science: carbon sheet solutions, Nature 442 (7100) (2006) 254–255.
[17] C. Lee, X.D. Wei, J.W. Kysar, J. Hone, Measurement of the elastic properties and intrinsic strength of monolayer graphene, Science 321 (5887) (2008) 385–388.
[18] K.S. Novoselov, A.K. Geim, S.V. Morozov, D. Jiang, Y. Zhang, S.V. Dubonos, A.A. Firsov, Electric field effect in atomically thin carbon films, Science 306 (5696) (2004) 666–669.
[19] R.F. Service, Graphene recipe yields carbon cornucopia, Science 322 (5909) (2008). 1785–1785.
[20] S.J. He, B. Song, D. Li, C.F. Zhu, W.P. Qi, C.H. Fan, A graphene nanoprobe for rapid, sensitive, and multicolor fluorescent DNA analysis, Adv. Funct. Mater. 20 (3) (2009) 1–7.
[21] C.X. Guo, X.T. Zheng, Z.S. Lu, X.W. Lou, C.M. Li, Biointerface by cell growth on layered graphene artificial peroxidase-protein nanostructure for in situ quantitative molecular detection, Adv. Mater. 22 (10) (2010) 5164–5167.
[22] M.S. Hizir, N.M. Robertson, M. Balcioglu, E. Alp, M. Rana, M.V. Yigit, Universal sensor array for highly selective system identification using two-dimensional nanoparticles, Chem. Sci. 8 (2017) 5735–5745.
[23] B.W. Liu, Z.Y. Sun, X. Zhang, J.W. Liu, Mechanisms of DNA sensing on graphene oxide, Anal. Chem. 85 (2013) 7987–7993.
[24] M.S. Hizir, N. Nandu, M.V. Yigit, Homologous miRNA analyses using a combinatorial nanosensor array with two-dimensional nanoparticles, Anal. Chem. 90 (2018) 6300–6306.
[25] C.Y. Zhou, C.T. Wu, D.L. Liu, Y.Q. Liu, E.K. Wang, An enzyme-free and DNA-based Feynman gate for logically reversible operation, Chem. Commun. 51 (51) (2015) 10284–10286.
[26] C.Y. Zhou, D.L. Liu, C.T. Wu, Y.Q. Liu, E.K. Wang, Integration of DNA and graphene oxide for the construction of various advanced logic circuits, Nanoscale 8 (40) (2016) 17524–17531.
[27] L. Wang, J. Zhu, L. Han, L. Jin, E.K. Wang, S.J. Dong, Graphene-based aptamer logic gates and their application to multiplex detection, ACS Nano 6 (8) (2012) 6659–6666.
[28] C.Y. Zhou, D.L. Liu, S.J. Dong, Innovative bimolecular-based advanced logic operations: a prime discriminator and an odd parity checker, ACS Appl. Mater. Interfaces 8 (8) (2016) 20849–20855.
[29] C.Y. Zhou, C.T. Wu, Y.Q. Liu, E.K. Wang, Effective construction of a AuNPs–DNA system for the implementation of various advanced logic gates, RSC Adv. 6 (108) (2016) 106641–106647.
[30] C.Y. Zhou, D.L. Liu, C.T. Wu, S.J. Dong, E.K. Wang, Multifunctional graphene/DNA-based platform for the construction of enzyme-free ternary logic gates, ACS Appl. Mater. Interfaces 8 (44) (2016) 30287–30293.
[31] S.L. Xu, H.L. Li, Y.Q. Miao, Y.Q. Liu, E.K. Wang, Implementation of half adder and half subtractor with a simple and universal DNA-based platform, NPG Asia Mater. 5 (2013) e76.

[32] M.X. You, L. Peng, N. Shao, L.Q. Zhang, L.P. Qiu, W.H. Tan, DNA "nano-claw": logic-based autonomous cancer targeting and therapy, J. Am. Chem. Soc. 136 (4) (2014) 1256–1259.
[33] Z.Z. Huang, H.N. Wang, W.S. Yang, Glutathione-facilitated design and fabrication of gold nanoparticle-based logic gates and keypad lock, Nanoscale 6 (14) (2014) 8300–8305.
[34] A. Ogawa, M. Maeda, Easy design of logic gates based on aptazymes and noncrosslinking gold nanoparticle aggregation, Chem. Commun. 31 (2009) 4666–4668.
[35] Z.Q. Guo, P. Zhao, W.H. Zhu, X.M. Huang, Y.S. Xie, H. Tian, Intramolecular charge-transfer process based on dicyanomethylene-4H-pyran derivative: an integrated operation of half-subtractor and comparator, J. Phys. Chem. C 112 (17) (2008) 7047–7053.
[36] S.Q. Zhang, K. Wang, C.C. Huang, Z.Y. Li, T. Sun, D. Han, A label-free and universal platform for the construction of an odd/even detector for decimal numbers based on graphene oxide and DNA-stabilized silver nanoclusters, Nanoscale 9 (33) (2017) 11912–11919.
[37] W.S. Hummers, R.E. Offeman, Preparation of graphitic oxide, J. Am. Chem. Soc. 80 (1958). 1339–1339.